Journal of Long-Term Effects of Medical Implants, 10(1&2):47–68(2000)

Stent-Based Gene Therapy

Marc D. Feldman M.D.,[1] Bo Sun, M.D.,[2] Bryan J. Koci, M.S.,[2] Clarence C. Wu, M.S.,[2] James R. Kneller, M.S.,[3] Harvey S. Borovetz, Ph.D.,[3] Simon Watkins, Ph.D.,[2] Ahmed Nadeem, M.S.,[3] Lee E. Weiss, Ph.D.,[4] Michael L. Reed, Ph.D.,[5] A. J. Conrad Smith, M.D.,[2] and Warren D. Rosenblum, M.D.[2]*

[1]Division of Cardiology, University of Texas Health Science Center in San Antonio, 7703 Floyd Curl Drive, San Antonio, Texas 78284-7872; [2]Department of Medicine, University of Pittsburgh School of Medicine; [3]Department of Biomedical Engineering, University of Pittsburgh School of Engineering; [4]Department of Electrical and Computer Sciences, Carnegie Mellon University; [5]Department of Electrical and Computer Sciences, University of Virginia

*Author to whom all correspondence should be addressed

Manuscript accepted in revised version: November 10, 1999

ABSTRACT: Delivery of gene therapy to inhibit intimal hyperplasia has been proposed to prevent postangioplasty restenosis. We sought to apply gene therapy by using a stent-based technique. There are several hurdles that must be overcome before gene-stent therapy can be applied successfully in clinical trials. These include increasing the efficiency of gene delivery through atherosclerotic plaque; increasing intramural retention times; preventing the inflammatory reaction that stents coated with biodegradable polymers can elicit; overcoming the risk of systemic gene delivery; and accessing the adventitia via percutaneous approach. We evaluated a gene-stent delivery mechanism based on microporous metal microneedles developed with nanotechnology in an attempt to overcome some of these problems.

A novel approach to the transfection of genes by microfabricated technology was evaluated in smooth muscle cells in culture. We demonstrated that microneedles can deliver gene therapy to smooth muscle cells in culture and can produce controlled penetration of the IEL and intima. We conclude that taller microneedles need to be developed to reach the media in diseased human arteries and that this technology has the potential to be incorporated in a stent to deliver gene therapy in atherosclerotic plaque.

KEYWORDS: Cells, genes, smooth muscle cells, plaque, restenosis.

I. INTRODUCTION

Coronary restenosis following intervention remains an area of active investigation.

1050-6934/00 $5.00

One proposed treatment to prevent and/or treat restenosis is the delivery of gene therapy to inhibit intimal hyperplasia. Previous investigators have been successful at delivering gene therapy to *in vivo* blood vessels by direct gene transfer to the arterial wall.[1-3] More recently, local application of gene therapy to injury models of intimal hyperplasia has been shown to either inhibit[4] or enhance[5,6] this process.

Early success with intimal hyperplasia models engendered great expectations for the potential of gene therapy as a possible solution to coronary restenosis. As a result, a clinical trial (ITALICS) of stent placement followed by c-myc antisense oligonucleotide delivered by catheter (Scimed, Minnesota) for the inhibition of intimal hyperplasia has been completed.[7] However, the ITALICS trial showed no benefit by clinical, angiographic, or intravascular ultrasound parameters. It is unclear whether this was due to failure of gene therapy or to other reasons.[8] The failure of this trial as the first attempt to examine gene therapy in combination with stent placement was predictable. There are still many issues to be resolved before gene therapy can be applied clinically with the expectation of successful outcome. Specifically, there are 5 hurdles yet to be overcome:

- ***The efficiency of gene delivery to vascular tissues is currently too low.*** Studies of delivery devices report fractional intramural delivery (ratio of intramural delivery mass to total delivered mass) of 0.1–1.0% in normal coronary arteries.[9-11] The atherosclerotic plaque represents a barrier that further reduces fractional intramural delivery. Feldman et al.[12] demonstrated that atherosclerosis reduced the transfection efficiency of adenoviral-mediated transfection 10-fold. Similarly, French et al.[13] noted a nearly 4-fold reduction in delivery of a recombinant adenovirus expressing luciferase activity in the arteries of cholesterol-fed and/or balloon-injured animals compared to arteries of normal animals. Finally, although Simari et al.[14] achieved successful transfection through atherosclerotic plaque and inhibited restenosis, gene expression was only prominent along the dissection plane created by the initial balloon injury. In summary, the development of a method to penetrate plaque in a predictable fashion to deliver bioactive agents into the media and adventitia is needed.
- ***The intramural retention times are too short.*** Brief exposure prevents the bioactive agent from exerting a biological effect.[15] In the restenotic process, the greatest decrease in luminal diameter occurs from weeks to months. The retention time of most locally delivered bioactive agents is hours to days. For instance, the retention time for heparin has been shown to be approximately 48 h in animal models[16,17] and patients.[18] To prolong retention times, controlled release matrices have been developed, mostly consisting of microparticles of biodegradable polymers that can be impregnated with drugs. However, using this approach, the retention time of Colchicine was only 24 h,[10] and some of the breakdown products can incite an inflammatory reaction.[19] One exception may be agents such as modified oligonucleotides with cell binding properties. They

persist up to 2 weeks following transfection, which is still short of the retention times required.[20]

- ***Stents coated with biodegradable drug-impregnated polymers can incite inflammatory reaction.*** Because of their mechanical effects, stents antagonize the elastic recoil and adventitial remodeling components of restenosis but do not affect intimal hyperplasia. This makes stents a suitable platform for sustained drug or gene administration, targeted to the intimal hyperplasia. Unfortunately, the polymers used as carriers can produce a marked inflammatory effect.[22] This has been partially overcome by the addition of dexamethasone to high density poly-L-lactic acid. However, the same material at a lower density still incited inflammatory reaction.[23] An alternative carrier that does not induce inflammatory reaction is fibrin-covered stents,[24] but their application to patients is problematic because the fibrinogen used is from human donors. Because metal stents have an excellent track record of being biocompatible and not inducing inflammatory reaction even after years of evaluation, the development of a drug-delivery metal stent is an attractive possibility.
- ***Bioactive agent delivery strategies still suffer from the risk of systemic distribution.*** Studies that have successfully delivered intramural agents, including viral vectors via intramural approach, have relied on surgically isolating the arterial segment, side branches, or both. However, this approach cannot be applied percutaneously. Use of new percutaneous delivery devices such as microporous balloons, which can typically deliver volumes of 2 ml, has demonstrated that only 2.5% of radiolabeled proteins are deposited locally, and the remainder is distributed systemically.[25] This would be of concern if viral vectors were used. March and coworkers[26] have detected luciferase expression as well as PCR-detected vector DNA in multiple tissues in the rabbit atherosclerotic model. Although other investigators have not confirmed this degree of systemic distribution,[27] the development of a method to achieve greater local delivery is essential.
- ***The ability to access the adventitia via percutaneous approach needs to be further developed.*** Remodeling is an important component of restenosis and is hypothesized to be based in the adventitia. The activation of adventitial myofibroblasts by mechanical injury appears to result in local production of scar tissue, resulting in vessel shrinkage and restenosis. The only percutaneous methods to access the adventitia are the needle catheter[28] and the nipple or infiltrator balloon.[29] Less traumatic and more precise delivery devices need to be developed.

Stent placement simplifies the biology of restenosis by being a pure model of intimal hyperplasia. Therefore, it is reasonable that gene therapy in patients should be delivered by stents. Accordingly, we propose the development of a gene-stent to overcome many of the hurdles outlined above.[30,31] Our proposed device is a gene-stent studded with microneedles whose tips are sharp and can cut through atherosclerotic plaque to gain access to the media and adventitia (Figure 1). These

microneedles are microporous to hold bioactive agents by surface tension, prolonging intramural retention times. Because the proposed device is entirely metallic, problems encountered with biodegradable polymers causing inflammatory reactions are presumably overcome. Because any viral vectors used are delivered slowly by the microporous needles, the risk of systemic exposure is minimized. These microneedles are produced by nanotechnology, which is used to introduce DNA into cells by microinjection needles.[32,33] Microneedles are potentially less traumatic than the needle catheter or the infiltration balloon. Finally, because the microneedles are based on a stent, their effect is aimed at delivering gene therapy to the intimal hyperplasia, seemingly the sole reason for stent restenosis.[8]

This research shows that stent-based microneedles can deliver gene therapy to smooth muscle cells in culture and that they can produce controlled penetration through the internal elastic lamina and hyperplastic intima, which constitute major barriers to the delivery of bioactive agents to diseased vessels.

II. METHODS

Microneedles used in this study were fabricated by reactive ion etching (RIE) of silicon.[34] The silicon substrate, which was thermally oxidized to grow a 1.5-mm layer of SiO_2, was sputter-coated with a 6000Å layer of aluminum. UV-photolithography was used to print arrays of circular patterns representing the location of the probes onto the aluminum layer. The substrate was then immersed into a mixture of phosphoric, nitric, and acetic acids (4:1:4). Areas of aluminum that were not protected by a photosensitive polymer coating were etched out, transferring a negative of the patterns onto the silicon substrate. The remaining aluminum pattern formed a protective mask for the silicon etch. Reactive ion etching of silicon was performed with a mixture of SF_6 and O_2 gas in 25:1 ratio. This gas ratio pro-

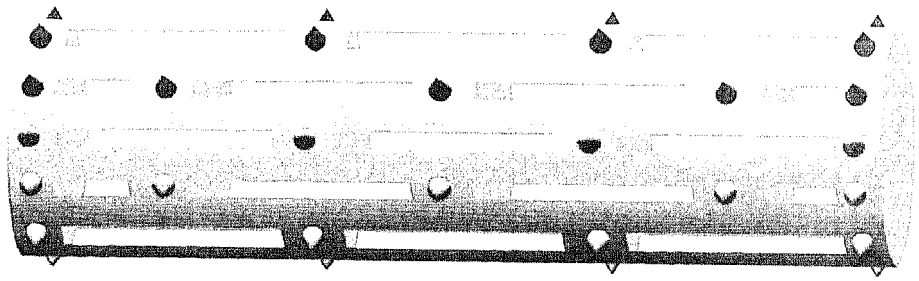

FIGURE 1. Conceptual depiction of a gene-stent. The surface of this metallic stent will be studded with microneedles. (The microneedles in this drawing are not to scale.)

duced the desired lateral and horizontal etch rate to form a pointed microstructure approximately 20 μm high. After an average etching time of 85 min, the substrate was thoroughly cleaned and 6000Å of platinum was sputtered on the substrate to improve DNA adhesion to the microneedle surface.

Using this fabrication process, microneedles with spacing of 40, 60, and 100 μm apart were produced on separate wafers (Figure 2). Increasing microneedle density was developed to test the hypothesis that the higher the density, the greater the smooth muscle cell transfection. The mean microneedle height was 20 ± 5 μm, and the mean tip size was 0.4 ± 0.1 μm ($n = 6$). This is similar to the size range of the micropipette tips used to inject DNA into single cells.[32,33] For studies of microneedle penetration into normal and atherosclerotic vessel walls, additional microneedles were developed using similar fabrication methods. These microneedles were 65 ± 15 and 140 ± 20 mm tall, had tip diameters of ≤ 3 mm, and had tip-to-tip distances of approximately 300 and 500 mm, respectively. Density, tip size, and height measurements were made with a scanning electron microscope.

II.A. Cell Culture

Vascular smooth muscle cells were obtained from the thoracic aortas of adult Sprague–Dawley rats with modifications of a previously reported method.[35] Aortas were blunt dissected to remove fat and adventitia, minced, digested for 90 min at 37 °C in DMEM/F12 containing 2 mg/ml bovine serum albumin (Sigma, St. Louis, Missouri), 0.25 mg/ml soybean trypsin inhibitor (Sigma), 0.125 mg/ml elastase (Type I, Sigma), and 1.0 mg/ml collagenase (Worthington, Newark, New Jersey). After filtration (70 μ nylon mesh), cells were plated on untreated 12 well plates at 3×10^5 cells/ml in DMEM/F12 (Gibco, Grand Island, New York), 10% fetal bovine serum (Paragon, Baltimore, Maryland), 10 mmol/L (mM) HEPES, 1 mmol/L (mM) glutamine, 100 U/ml penicillin (Paragon, Baltimore, Maryland), 100 ug/ml streptomycin (Paragon), 0.5μg/ml gentamicin, and 0.5μg/ml amphotericin B (Mediatech, Herdon, Virginia) and grown in 5% CO2 at 37 °C. At confluence, cells were removed with 0.25% trypsin (Life Sciences, Denver, Colorado) and replated. Transfection studies were performed using cells between the 1st and 4th passage. We previously performed immunostaining with a monoclonal antibody sensitive to smooth muscle a-actin (Sigma) to confirm the predominant cell type to be vascular smooth muscle.

II.B. Plasmid Isolation

Propagation of pIEPLacZ (7.0kb CMV promoter) plasmid was obtained from the

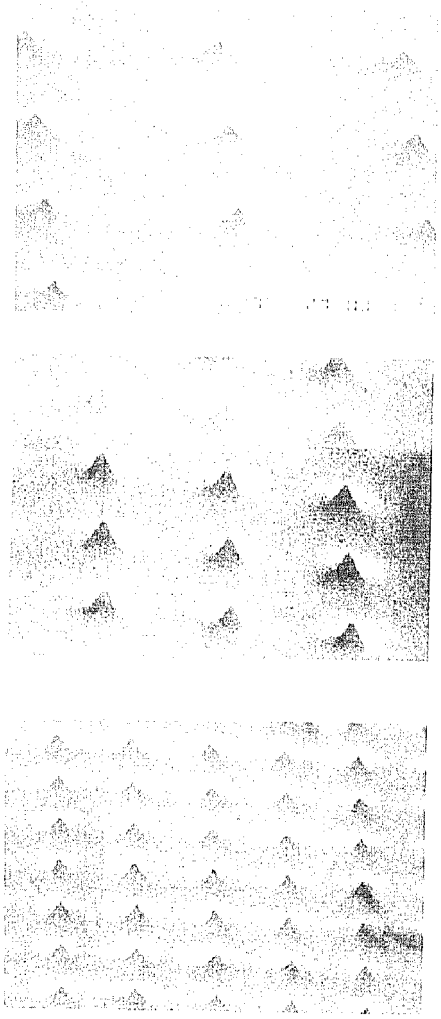

FIGURE 2. Micrographs of the microneedles. Scanning electron microscopy was used to generate these micrographs of microneedles with spacing of 100 (top), 60 (middle), and 40 (bottom) μm, etched on silicon wafers sputter-coated with aluminum. The mean tip size was 0.4 ± 0.1 μm, and mean height was 20 ± 5 μm. The bar is 100 μm. All micrographs are at the same magnification.

bacterial strain DH5α using 50 μg/ml of ampicillin in LB medium. DNA was isolated and purified via a plasmid kit (Qiagen-tip 2500, Mega, Quiagen, Santa Clarita, California).

III.C. Transfection of Cells with Microneedles

A custom designed apparatus was used to centrifuge DNA onto the microneedles. The silicon wafers, each coated with different densities of microneedles, were cleaved into $1 cm^2$ pieces and bonded onto the apparatus. There is a removable reservoir over the microneedles to which solutions can be added and centrifuged. The microneedles were pretreated in the apparatus with 200 μl of 0.1M spermidine at 22 °C for 10 min. This solution was replaced with the DNA precipitation mixture consisting of 40 μg of DNA, 400 μl of 0.25 M $CaCl_2$, and 200 μl of 0.1M spermidine incubated at 22 °C for 10 min. The mixture, reservoir, and microneedles were centrifuged at 4500 RPM at 4 °C for 1 h. The mixture and reservoir were removed and the microneedles washed with 100% ethanol and allowed to air dry. The washing procedure was repeated with 70% ethanol. Prior to transfection, the probes were presoaked in 1 ml of dd H_20 for 2 min to remove residual salt. After this, the DNA retained by the microneedles was 6.7 ± 0.6 μg, as confirmed by spectrophotometry.

The microneedle assembly was inverted and applied to the smooth muscle cells in culture. A 100-g weight was placed on top of the apparatus to provide driving force to pierce the cells. The apparatus was removed after 4 min, and 1 ml of fresh medium was added to the wells. After 24 h, the cells were washed and replenished with 2 ml of fresh media. The cells were then grown for 24 h before staining for LacZ. The same procedure was used for all microneedle densities.

II.D. Calcium phosphate-DNA precipitation

To compare microneedle cell transfection efficiency to standard techniques, we also examined calcium phosphate[36,37] and liposome[38-40] transfection methods. Before the transfection procedure, media from the cultured cells was removed and replaced with 1 ml of fresh medium. A solution of 150 μl of 0.25 M $CaCl_2$ and 150 μl of 2xBBS (50mM BES, 1.5mM Na_2HPO_4, 80mM NaCl, pH 6.95) along with 5 μg of plasmid DNA were mixed together and incubated for 15 min at 37 °C. Calcium-phosphate DNA solution (300 μl) was added dropwise to each well, swirling to mix. The cells were incubated overnight and then washed with phosphate-buffered solution (PBS). Fresh medium (2 ml) was added to the cells and incubated for a further 24 h before gene expression was analyzed.

II.E. Liposome Transfection

Positively charged polycationic liposomes (LipofectAmine reagent, Gibco) containing

2,3–dioleyloxy–N–[2(spermine-carboxamido)ethyl]–N–demethyl–1–propanaminium-trifluoroacetate (DOSPA) and the neutral lipid dioleoyl phosphatidylethanolamine (DOPE) were used in the liposome transfections. Prior to transfection, the cells were washed with serum-free medium, and 1 ml of the serum-free medium was added to the wells. Plasmid DNA (1 μg) was diluted into 200 μl of serum-free media, and LipofectAmine (4 μl) was mixed with 200 μl of serum-free media. The 2 solutions were mixed and incubated for 15 min at room temperature. The existing medium was removed, and LipofectAmine/DNA complex (400 μl) was added to the cells. After 4 h, the transfection mixture was removed and replaced with 2 ml serum-supplemented medium. The cells were allowed to grow for 48 h, then examined for ß-galactosidase expression.

II.F. Analysis of Gene Expression

ß-galactosidase expression was assessed, as previously described.[41] The existing media was removed, and the cells were washed with PBS. Cells were fixed with 1 ml of ice-cold paraformaldehyde (4%) and incubated at 4 °C for 15 min. Cells were incubated for 4 h at 37 °C in the reaction mixture 5–bromo–4–chloro–3–indoyl–ß–D–galactoside chromogen (X-gal, 8 mg/ml) in 200 μl of DMSO, potassium ferricyanide (10 mmol/L), potassium ferrocyanide (10 mmol/L), and 6.8 ml Tris-buffered saline (TBS) (pH 8.0). The blue-stained cells were counted in 5 sample regions. Results between groups were compared by one-way ANOVA with Tamhame post-hoc test. Regional distribution differences were analyzed by calculating the variance of every well and comparing each treatment using Levene's test for equal variances.

II.G. Isolated Iliac Arteries

Ten iliac arteries, removed from 5 normal and 5 atherosclerotic New Zealand white rabbits (6 months to 2 years old, 3–4 kilograms) were used in this study. The protocol was approved by the Institutional Animal Care and Use Committee of the University of Pittsburgh and conformed to the National Institutes of Health Guidelines for Use of Animals in Research. The rabbit model of atherosclerosis developed by Block et al.[42] and Faxon et al.[43] was used. The atherosclerotic lesions were created by feeding the rabbits a diet containing 5% cholesterol and 7% peanut oil for 3 weeks. Arterial balloon injury to the iliac artery was then performed with a 2F Fogarty catheter, and the hypercholesterolemic diet was resumed for another 3–5 weeks.

Because microneedles are ultimately intended to be deployed by an intravas-

cular stent, clinical conditions were simulated. Stent deployment in patients results in 10–30% circumferential vessel distention. The intraluminal pressures corresponding to this degree of distention may be determined from previous compliance measurements of normal and atherosclerotic rabbit arteries.[44] The intraluminal pressure range (ΔP) needed to distend the artery during stenting is related to its compliance (C) and to the volume change (ΔV) of the vessel by Equation 1:

$$\Delta P = \Delta V / C \tag{1}$$

For normal and atherosclerotic rabbit vessels, the compliance values were reported to be 0.058×10^{-3} and 0.061×10^{-3} ml/mmHg, respectively.[44] Assuming a unit length of vessel and a concentric atherosclerotic lesion, and using the mean diameter of rabbit iliac arteries previously determined,[45] these compliance values correspond to intraluminal pressures ranging from 143 to 500 mm Hg. Based on these calculations, pressures of 100, 300, and 500 mmHg were used in this study.

To harvest the iliac arteries, rabbits were sedated with 5 mg/kg sq xylazine (Miles, Shawnee Mission, Kansas) and 0.1 mg/kg atropine (Liphomed, Deerfield, Illinois) followed by general anesthesia with 40 mg/kg i.v. ketamine (Fort Dodge Lab., Fort Dodge, Iowa) and 0.1 mg/kg acepromazine (Aveco, Fort Dodge, Iowa). The tissue handling protocol developed by Fry et al.[46-48] for filleted arteries *in vitro*

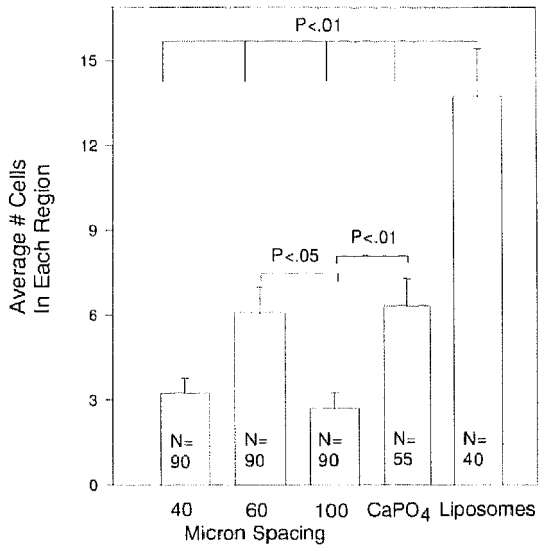

FIGURE 3. Transfection efficiency for all methods. Among the microneedles, the 60-μm spacing had the highest average cells/region, 2-fold greater than the 40- and 100-μm spacing. The 60-μm microneedle density was as efficient as the $CaPO_4$ method, but less efficient than liposomes.

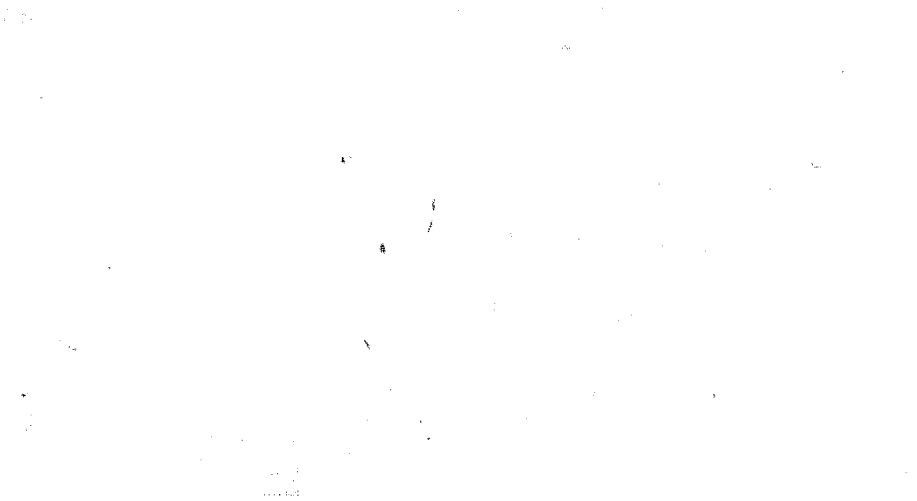

FIGURE 4. Regional differences in transfection. Photomicrographs of smooth muscle cells in culture with blue-stained nuclei consistent with ß-galactosidase expression are shown. The left panel was transfected with 60-µm spacing microneedles and shows regional expression, while the middle ($CaPO_4$) and right (liposomes) panels show more uniform expression.

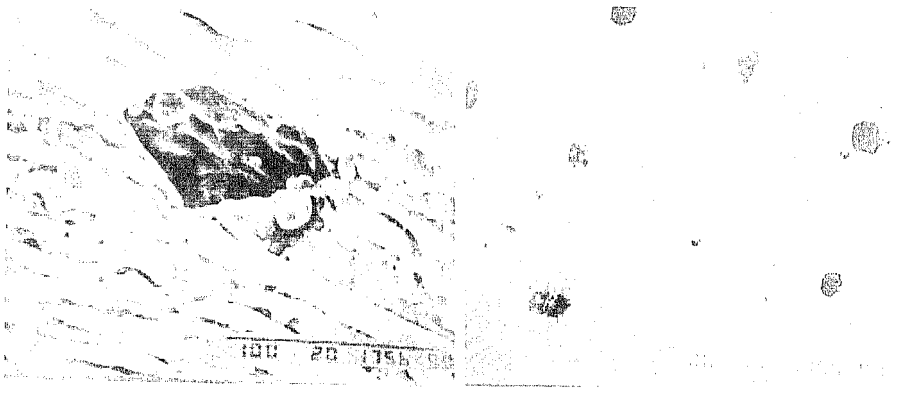

FIGURE 5. Scanning electron micrograph of a typical single microneedle penetration hole (left) and group of penetrations (right) of a normal rabbit iliac artery with preservation of the surrounding endothelial surface. The bars represent 100 µm.[65]

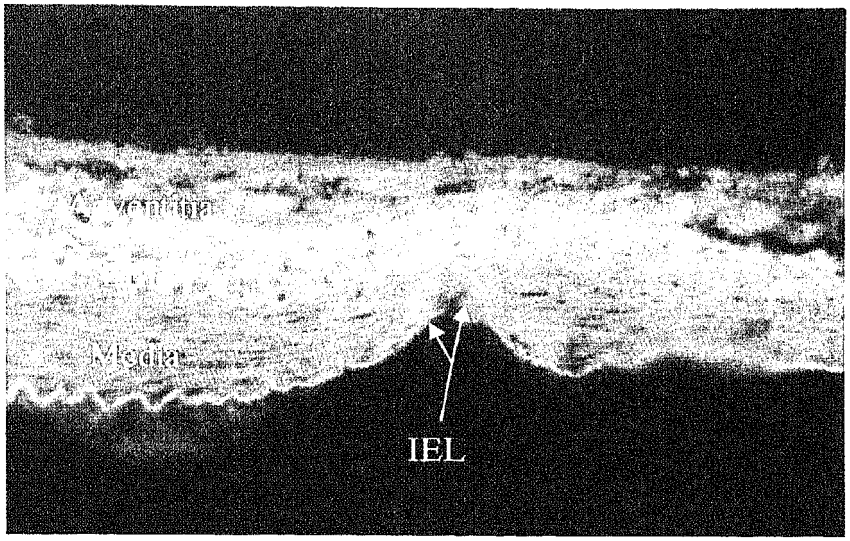

FIGURE 6. The mechanism of IEL penetration with the 140 ± 20-μm tall microneedles in an iliac artery is shown. Light microscopy superimposed with fluorescence microscopy image demonstrates that the cut ends of the IEL (arrows) remain adjacent to the site of penetration.[30]

was followed. Both iliac arteries were dissected from the distal side of the inguinal ligament to the abdominal wall. The base of the aorta was ligated to allow cannulation of the iliac branch, permitting pressure perfusion with medium to rinse the vessel free of blood. The vessel was opened longitudinally along its dorsal aspect, and clamped as a flat sheet, according to the methods of Brant et al.[49] Following removal, the vessel was bathed in Cellgro™ 199 *in vitro* Cell Culture medium (Mediatech, Herdon, Virginia) at 37 °C. Harvested arterial segments were mounted luminal side up on a tissue holding device. The original circumference of the artery was then restored by 1.4-fold distension with a tissue-stretching device.[50] The artery's final circumference ranged from 0.795 to 0.939 cm.

The microneedles, iliac artery, and tissue stretching device were lowered into a tissue-holding chamber. The microneedles were then applied to the vessel lumen and pressure applied. Pressure was monitored via a fluid-filled transducer. During pressure application, the media was removed and replaced with 2.5% glutaraldehyde in phosphate buffer for 20 min to preserve the microneedle–tissue interactions. The microneedles were removed and the tissue fixed for an additional 60 min.

II.H. Tissue Processing and Imaging

Scanning electron microscopy was used to evaluate microneedle interaction with the endothelial surface. Tissues were dehydrated using transmission electron microscopy protocol, then pinned to wax wafers. The samples were dried in a thermoelectric critical point dryer (Emscope CPD 750, Erie, Pennsylvania) and placed in a specimen chamber with 100% ethanol. A series of soaking and venting steps with CO_2 were performed until no ethanol could be detected. The chamber temperature was raised from 10 to 40 °C to dry the specimens. Dried tissue was sputter-coated with gold and palladium (Technics Hummer VI) and placed on aluminum mounting platforms. Samples were then placed in the sample chamber and imaged (Jeol JSM-T300, Peabody, Massachusetts).

Light superimposed with fluorescence microscopy was used to quantitate IEL and EEL penetration and plaque compression by the microneedles. Samples were transferred from the fixative to 30% sucrose for 24 h, then frozen in isopentane chilled in liquid nitrogen. Following sectioning, normal iliac arteries were stained with hematoxylin and eosin. Atherosclerotic iliac arteries were stained with Oil red O-isopropanol with hematoxylin as a counterstain. Both vessel types were imaged with a light microscope. A fluorescence microscope was used to auto-fluoresce the IEL and EEL. The fluorescence image was superimposed on the light field image to determine if the IEL and EEL had been penetrated. Penetration was defined as cell nuclei at 90° to an adjacent microprobe tip. Compression was defined as cell nuclei parallel to an adjacent microneedle tip.

III. RESULTS

III.A. Expression of ß-Galactosidase in Rat Aortic Smooth Muscle Cells

A summary of the transfection efficiency by ß-galactosidase encoded plasmid using microneedles, $CaPO_4$, and liposomes is found in Figure 3. The number of LacZ positive stained cells per region with 40 μm density microneedles (3.2 ± 0.54) was comparable with 100 μm density microneedles (2.7 ± 0.54). The 60 μm density microneedles had the highest average number of cells per region (6.1 ± 0.92), which was 2-fold greater than that obtained with 100 μm density microneedles($p < 0.05$). The 60 μm density microneedles were as efficient as the $CaPO_4$ method (p = NS).

Controls revealed that when 10 μg plasmid DNA was added to the wells, transfection did not occur ($n = 18$). When 10 μg plasmid DNA was added directly to the well and the 40-, 60-, and 100-μm density microneedles were applied, transfection

did not occur ($n = 11$). Finally, when 10 μg plasmid DNA was added directly to the well and silicon wafers without microneedles were applied, transfection did not occur ($n = 4$).

Transfection using liposomes with a plasmid containing pIEPLacZ yielded the greatest number of positive nuclei containing nuclear ß-galactosidase expression. When liposomes were compared with microneedles and $CaPO_4$, the liposome method had a significantly greater number of stained cells per region ($p < 0.01$, Figure 3). Liposome efficiency was 2× greater than were $CaPO_4$ and 60 μm, and 4× greater than were the 40- and 100-μm spaced microneedles.

III.B. Variability in Transfection Efficiency

To investigate the possibility that regional distribution of stained cells among the 3 methods of transfection was different, we calculated the variance of the 5 sampled regions in each well, for each method. The microprobes were found to have a greater variability of transfected nuclei than both chemical methods. The variance of the 60-μm spaced microprobes was greater than that of the $CaPO_4$ method ($p < 0.01$) and the liposome method ($p < 0.05$). The variance of the $CaPO_4$ method was also lower than the liposome method ($p < 0.01$). The average variance of the 60-μm spaced probes was 32 ± 8, the liposomes 21 ± 5, and the $CaPO_4$ 10 ± 2.

III.C. Microneedle Penetration into Normal, Isolated Rabbit Iliac Arteries

Multiple microneedle penetrations and a representative single microneedle penetration at higher magnification (Figure 5) show that endothelial cells are only disrupted at the site of microneedle contact, with no damage to surrounding endothelium.[65] The incidence of IEL penetration for the 2 types of microneedles at the 3 pressures examined is summarized in Table 1. The 65 ± 15 mm sharp microneedles compressed but did not penetrate the IEL into the media in all 34 samples, at 100, 300, and 500 mm Hg of pressure. The 140 ± 20 mm microneedles penetrated the IEL in all 24 samples at all pressures, without disruption. An example is shown in Figure 6.

EEL penetration was also evaluated for both microneedle sizes at similar pressures, and 34, 65 ± 15 mm microneedles did not penetrate the EEL at any pressure. However, 2 of 24, 140 ± 20 mm microneedles did penetrate the EEL, but only at 500 mm Hg pressure.

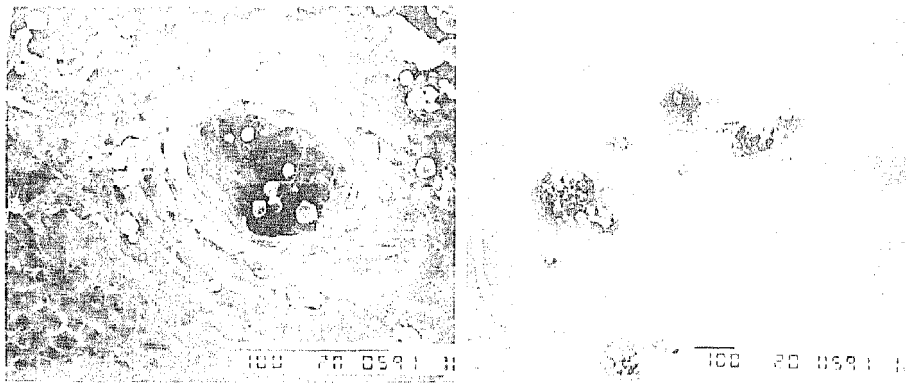

FIGURE 7. Scanning electron micrograph of a representative single microneedle penetration (left) and group of 4 penetrations (right) in an atherosclerotic rabbit iliac artery. Disruption of the plaque is limited to the site of microneedle contact. Bars are 100 μm.[65]

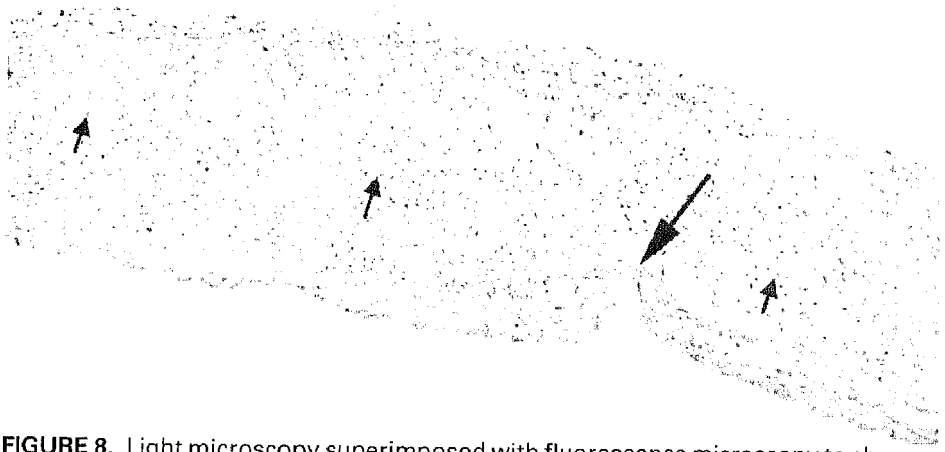

FIGURE 8. Light microscopy superimposed with fluorescence microscopy to show an example of 140 ± 20 microneedle plaque penetration in an isolated atherosclerotic rabbit iliac artery. Large arrow identifies microneedle penetration. Small arrows indicate the IEL. The microneedles used in this study were not tall enough to penetrate through the plaque to the media.

III.D. Microneedle Penetration in Isolated, Atherosclerotic Rabbit Iliac Arteries

The 140 ± 20 mm microneedles penetrated into the hyperplastic intima, as shown in Figure 7. Disruption of the plaque was only at the site of microneedle contact.

The 65 ± 15 mm microneedles that did not penetrate the IEL of normal arteries were not included. The 140 ± 20 mm microneedles compressed the plaque in all 20 examined samples, at the 3 pressures applied. IEL penetration, however, was present in only 1 out of 20 examined samples, and only at 500 mm Hg of pressure. There were no instances of EEL penetration. Figure 8 shows that the microneedles used in this study were not tall enough to penetrate through the plaque to the media.

IV. DISCUSSION

The ultimate goal of this project is to develop a porous microneedle-studded stent to deliver gene therapy in conjunction with coronary intervention. This study has confirmed that microneedles can successfully transfect genes into smooth muscle cells in culture. There was a significant increase in cell transfection by increasing microneedle spacing from 100 to 60 μm. However, a further increase in microneedle density from 60 to 40 μm resulted in a decrease in transfection efficiency. The transfection efficiency of the 60 μm spacing microneedles was equal to a standard technique to transfect cells in culture, $CaPO_4$, although not equal to liposomes. Among the different densities examined, 60 μm microneedle spacing is optimal.

There was significant variance in microneedle transfection. For each of 5 regions observed over the 1 cm^2 wafer that contacted the cells, there were regions lacking transfected cells, and other areas in the same well with significant transfection. Silicon wafers have no curvature, while the wells containing the smooth muscle cells had curvature. The curvature of the wells was estimated to be 2 ± 1

TABLE 1.
Incidence of IEL Penetration in Normal Vessels[65]

Microneedle	Pressure (mmHg)		
Group (mm)	100	300	500
65 ± 15	0 / 10	0 / 8	0 / 16
140 ± 20	7 / 7	7 / 7	10 / 10

n1 / n2 where n1 = number of positive occurrences, n2 = number of observations.

μm, while the microneedles were 20 ± 5 μm tall. This implies that 10% of the reach of the microneedles was lost in the curvature of the well. In contrast, the 2 chemical methods examined produced more uniform cell transfection, as was demonstrated in Figure 4, because they have access to every cell.

The mechanism of cell transfection is believed to be the result of direct injection of DNA into individual smooth muscle cells. First, we documented that 6.7 ± 0.6 μg of DNA was on the microneedle wafer immediately prior to applying it to the cells in culture. Second, microneedle tips were manufactured to be 0.4 ± 0.1 μm, similar in size to micropipette tips used to inject DNA into cells.[32,33] Third, it was demonstrated that the observed effect was not simply irritation of the cell membrane inducing endocytosis of DNA. Placement of DNA in solution outside the cells followed by application of microneedles without DNA or silicon wafers without microneedles did not result in any transfection of cells. Finally, there was an increase in cell transfection when microneedle density was increased from 100 to 60 μm. The decrease in transfection when microneedle density was increased further to 40 μm may be due to a greater proportion of cells' dying, although this was not documented.

The percentage of cells transfected by all 3 techniques was low, and consistent with previous literature on transfection efficiency of smooth muscle cells in culture.[39] Liposomes transfected 1.76% of cells while the 60-μm density microneedles and $CaPO_4$ transfected 0.78% and 0.81%, respectively. The low transfection rates in the current study are in part due to the smooth muscle cells in culture being at 100% confluence. After confluence, cell mitosis declines. Previous investigators have shown that mitotic smooth muscle cells in culture are preferentially transfected.[39] Nabel and coworkers[40] also demonstrated a decline in transfection efficiency when cells in culture had more than 90% confluence, and it was maximal at 75% confluence. However, we chose cultures with 100% confluence so that transfection by microneedles in direct contact with cells could be compared to $CaPO_4$ and liposomes. Another explanation for the low transfection efficiency reported from this and other studies, based on the use of LacZ gene transfer, is that histochemical staining (X-gal) underestimates transfection efficiency compared to newer immunostaining methods.[51]

This study has also demonstrated that microneedles developed with nanotechnology may cross barriers to local drug and gene therapy, the internal elastic lamina and intimal hyperplasia of experimental atherosclerotic plaque. For normal rabbit iliac arteries, the 65 ± 15 μm microprobes compressed, but were too short to penetrate, the IEL. The 140 ± 20-μm tall microprobes consistently penetrated the IEL and entered the media. The magnitude of the applied force influenced the degree of penetration of the EEL. The 140 ± 20-μm tall microprobes penetrated into the adventitia only when 500 mm Hg of pressure was applied. Taller microprobes consistently compressed the intimal, but they were rarely tall enough to penetrate the IEL and enter the media.

The needle catheter or the nipple balloon can cause excessive trauma while

penetrating vascular tissue barriers and can promote further development of atherosclerosis and restenosis. The ability of a delivery mechanism to preserve the IEL is underscored by the work of Sims[52,53] and Sims et al.,[54] who demonstrated that the greater incidence of arteriosclerosis in the coronary as compared to the internal mammary arteries is related to the integrity of the IEL. In autopsy specimens from 300 patients, they demonstrated that the mammary artery showed only minimal defects in the IEL at all ages, while the coronary arteries showed substantial defects in the IEL, which increased with age. Schwartz et al.[55,56] demonstrated that the mean intimal thickness in laboratory animals increases with the degree of laceration of the internal elastic lamina, and that intimal proliferative response near each break reflects the magnitude of the damage. Morimoto et al.[57] made similar observations in human restenosis. Therefore, a stent studded with microneedles could be a rational approach to delivering gene therapy while minimizing the extent of damage to the IEL.

Although the gene-stent delivery mechanism proposed in this manuscript overcomes many of the hurdles to gene therapy outlined in the introduction, there are limitations to this approach. Human plaque is often eccentric and has irregular surfaces. This implies that microneedles of constant height on a stent would not have access to every region of the media. However, a recent study by Mintz et al.[58] demonstrated that one consequence of balloon angioplasty is axial redistribution of plaque to relatively even proportions. Furthermore, microneedle-studded stents could be manufactured with microneedles of varying heights.

There are also limitations related to differences between human atherosclerosis and the rabbit model of neointimal hyperplasia. The stiffness of mature human plaque is greater than that of the plaque created in the rabbit model, devoid of calcification and fibrosis. Loree et al.[59] divided human plaques into 3 groups: cellular, hypocellular, and calcified, with circumferential tangential stiffness moduli of 927 ± 468 kPa, 2312 ± 2180 kPa, and 1466 ± 1284 kPa, respectively. A similar range was reported by Lendon et al.[60] Based on these figures, the intraluminal pressure needed to distend a concentric lesion by 30% ranges from 1209 to 3016 mmHg for these 3 types of human plaque. Consequently, the intraluminal pressures used in this study to simulate stenting are lower than those required for human atherosclerosis by a factor of 2.4 to 6.0. Furthermore, the microneedles tested were based on flat silicon wafers, which prevented the microneedles from full penetration. Microneedles based on cylindrical stents may be subject to a greater applied force to the vessel wall.

Tip designs on the microprobes can be altered to enhance DNA delivery. Porous tips can be microfabricated to hold more DNA than those tested in this study. Hollow tips can be microfabricated to inject DNA directly into the blood vessel. Because electrical fields are maximal at tips, and DNA is a charged particle, the ability to enhance transfection by adding iontophoresis to microneedles may enhance gene delivery. Iontophoresis has been used to transfect cells in culture[61] and enhance the delivery of proteins to the intact vasculature.[62] Finally, it may not be

necessary to directly pierce each medial smooth muscle cell in an intact blood vessel to achieve efficient transfection. Recent studies of ischemic limbs by Isner and coworkers[63,64] demonstrated that injection of nude plasmid DNA into skeletal muscle results in stable transfection.

V. CONCLUSION

In conclusion, this paper proposes a novel gene-stent delivery mechanism to overcome limitations to the clinical application of gene therapy to coronary restenosis. As preliminary proof of principle, we demonstrated that smooth muscle cells in culture could be transfected with microneedles. We also demonstrated that microneedles can produce controlled penetration through the internal elastic lamina and atherosclerotic plaque. Future studies will require the fabrication of a gene stent and will need to demonstrate that microneedles can actually deliver gene therapy to intact atherosclerotic blood vessels.

ACKNOWLEDGEMENT

This research was supported in part by R29HL-47046-01 (MDF).

REFERENCES

(1) Nabel, E. G., Plautz, G., and Nabel, G. J., Site-specific gene expression *in vivo* by direct gene transfer into the arterial wall, *Science*, **1990**, 249:1285–1288.

(2) Lim, C. S., Chapman, G. D., Gammon, R. S., Muhlestin, J. B., Bauman, R. P., Stack, R. S., and Swain, J. L., Direct *in vivo* gene transfer into the coronary and peripheral vasculature of the intact dog, *Circulation*, **1991**, 83:2007–2011.

(3) Flugelman, M. Y., Jaklitsch, M. T., Newman, K. D., Casscells, W., Bratthauer, G. L., and Dichek, D. A., Low-level *in vivo* gene transfer into the arterial wall through a perforated balloon catheter, *Circulation*, **1992**, 85:1110–1117.

(4) Chang, M. W., Barr, E., Seltzer, J., Jiang, Y. Q., Nabel, G. J., Nabel, E. G., Parmacek, M. S., and Leiden, J. M., Cytostatic gene therapy for vascular proliferative disorders with a constitutively active form of the retinoblastoma gene product, *Science*, **1995**, 267:518–522.

(5) Nabel, E. G., Yang, Z., Liptay, S., San, H., Gordon, D., Haudenschild, C. C., and Nabel, G. J., Recombinant platelet-derived growth factor B gene expression in porcine arteries induces intimal hyperplasia *in vivo*, *J. Clin. Invest.*, **1993**, 91:1822–1829.

(6) Nabel, E. G., Yang, Z. Y., Plautz, G., Forough, R., Zhan, X., Haudenschild, C. C., Maciag, T., and Nabel, G. J., Recombinant fibroblast growth factor–1 promotes intimal hyperplasia and angiogenesis in arteries *in vivo*, *Nature*, **1993**, 362:844–846.

(7) Ferguson, J. J., Meeting highlights: 20th congress of the european society of cardiology (ITALICS), *Circulation*, **1999**, 99:1130.

(8) DeYoung, M. B. and Dichek, D. A., Gene therapy for restenosis: are we ready? *Circ. Res.*, **1998**, 82:306–313.

(9) March, K. L. and Trapnell, B. C., Pharmacokinetics of local viral vector delivery to vascular tissues: Implications for efficiency and localization of transduction, in *Gene Transfer in the Cardiovascular System: Experimental Approaches and Therapeutic Implications*, March, K. L., Ed., Kluwer, 1997:477–498.

(10) Gradus–Pizlo, I., Wilensky, R. L., March, K. L., Fineberg, N., Michaels, M., Sandusky, G. E., and Hathaway, D. R., Local delivery of biodegradable microparticles containing colchicine analogue: Effects of restenosis and implications for catheter-based drug delivery, *J. Am. Coll. Cardiol.*, **1995**, 26:1549–1557.

(11) Muller, D. M., Topol, E. J., Abrams, G. D., Gallagher, K. P., and Ellis, S. G., Intramural methotrexate therapy for the prevention of neointimal thickening after balloon angioplasty, *J. Am. Coll. Cardiol.*, **1992**, 20:460–466.

(12) Feldman, L. J., Steg, P. G., Zheng, L. P., Chen, D., Kearney, M., McGarr, S. E., Barry, J. J., Dedieu, J. F., Perricaudet, M., Isner, J. M., Low efficiency of percutaneous adenovirus-mediated arterial gene transfer in the atherosclerotic rabbit, *J. Clin. Invest.*, **1995**, 95:2662–2671.

(13) French, B. A., Mazur, W., Ali, N. M., Geske, R. S., Finnigan, J. P., Rodgers, G. P., Roberts, R., and Raizner, A. E., Percutaneous transluminal *in vivo* gene transfer by recombinant adenovirus in normal porcine coronary arteries, atherosclerotic arteries, and two models of coronary restenosis, *Circulation*, **1994**, 90:2402–2413.

(14) Simari, R. D., Hong, S., Rekhter, M., Ohno, T., Gordon, D., Nabel, G. J., and Nabel, E. G., Regulation of cellular proliferation and intimal formation following balloon injury in atherosclerotic rabbit arteries, *J. Clin. Invest.*, **1996**, 98:225–235.

(15) Wilensky, R. L., Catheter-based local drug and gene delivery, in *Gene Transfer in the Cardiovascular System: Experimental Approaches and Therapeutic Implications*, March, K. L., Ed., Kluwer, 1997:180–199.

(16) Flugelman, M. Y., Jaklitsch, M. T., Newman, K. D., Casscells, W., Bratthauer, G. L., Dichek, D. A., Low-level *in vivo* gene transfer into the arterial wall through a perforated balloon catheter, *Circulation*, **1992**, 85:1110–1117.

(17) Azrin, M. A., Mitchel, J. F., Fram, D. B., Pedersen, C. A., Cartun, R. W., Barry, J. J., Bow, L. M., Waters, D. D., and McKay, R. G., Decreased platelet deposition and smooth muscle cell proliferation after intramural heparin delivery with a hydrogel-coated balloon, *Circulation*, **1994**, 90:433–441.

(18) Camenzind, E., Bakker, W. H., Reijs, A., van Geijlswijk, I. M., Boersma, E., Kutryk, M. J. B., Krenning, E. P., Roelandt, J. R. T. C., and Serruys, P. W., Site-specific intracoronary heparin delivery in humans after balloon angioplasty: A radioisotopic assessment of regional pharmacokinetics, *Circulation*, **1997**, 96:154–165.

(19) Brieger, D. and Topol, E., Local drug delivery systems and the prevention of restenosis, *Cardiovasc. Res.*, **1997**, 35:405–413.

(20) Wilensky, R. L., Catheter-based local drug and gene delivery, in *Gene Transfer in the Cardiovascular System: Experimental Approaches and Therapeutic Implications*, March, K. L., Ed., Kluwer, 1997:194.

(21) van der Giessen, W. J., Lincoff, M., Schwartz, R. S., van Beusekom, H. M. M., Serruys, P. W., Holmes, Jr., D. R., Ellis, S. G., and Topol, E. J., Marked inflammatory sequelæ to implantation of biodegradable and non-biodegradable polymers in porcine coronary arteries, *Circulation*, **1996**, 94:1690–1697.

(22) Murphy, J. G., Schwartz, R. S., Edwards, W. D., Camrud, A. R., Vlietstra, R. E., and Holmes, Jr., D. R., Percutaneous polymeric stents in porcine coronary arteries: Initial experience with polyethylene terephthalate stents, *Circulation*, **1992**, 86:1596–1604.

(23) Lincoff, A. M., Frust, J. G., Ellis, S. G., Tuch, R. J., and Topol, E., Sustained local delivery of

dexamethasone by a novel intravascular eluting stent to prevent restenosis in the porcine coronary injury model, *J. Am. Coll. Cardiol.*, **1997**, 29:808–816.

(24) McKenna, C. J., Camrud, A. R., Sangiorgi, G., Kwon, H. M., Edwards, W. D., Holmes, Jr., D. R., and Schwartz, R. S., Fibrin-film stenting in a procine coronary injury model: Efficiency and safety compared with uncoated stents, *J. Am. Coll. Cardiol.*, **1998**, 31:1434–1438.

(25) March, K. L. and Trapnell, B. C., Pharmacokinetics of local viral vector delivery to vascular tissues: Implications for efficiency and localization of transduction, in *Gene Transfer in the Cardiovascular System: Experimental Approaches and Therapeutic Implications*, March, K. L., Ed., Kluwer, 1997:483.

(26) March, K. L., Gradus–Pizlo, I., Wilensky, R. L., Yei, S., and Trapnell, B. C., Cardiovascular gene therapy using adenoviral vectors: Distant transduction following local delivery using a porous balloon catheter, *J. Am. Coll. Cardiol.*, **1994**, 23(1):177A.

(27) Steg, P. G., Feldman, L. J., Scoazec, J. Y., Tahlil, O., Barry, J. J., Boulechfar, S., Ragot, T., Isner, J. M., and Perricaudet, M., Arterial gene transfer to rabbit endothelial and smooth muscle cells using percutaneous delivery of an adenoviral vector, *Circulation*, **1994**, 90:1648–1656.

(28) Gonschior, P., Goetz, A. E., Huehns, T. Y., and Hofling, B., A new catheter for prolonged local drug application, *Coron. Artery Dis.*, **1995**, 6:329–334.

(29) Barath, P., Popov, A., Dillehay, G., Matos, G., and McKiernan, T., Infiltrator angioplasty balloon catheter: A device for combined angioplasty and intramural site-specific treatment, *Cathet. Cardiovasc. Diagn.*, **1997**, 41:333–341.

(30) Reed, M. L., Wu, C., Kneller, J., Watkins, S., Vorp, D. A., Nadeem, A., Weiss, L. E., Rebello, K., Mescher, M., Smith, A. J. C., Rosenblum, W., and Feldman, M. D., Micromechanical devices for intravascular drug delivery, *J. Pharm. Sci.*, **1998**, 87:1387–1394.

(31) Feldman, M. D., Kneller, J., Wu, C., Watkins, S., Weiss, L., and Reed, M., Microfabricated device for intravascular delivery, *J. Am. Coll. Cardiol.*, **1998**, 31(2):351A.

(32) Gordon, J. W., Scangos, G. A., Plotkin, D. J., Barbosa, J. A., and Ruddle, F. H., Genetic transformation of mouse embroys by microinjection of purified DNA, *Proc. Natl. Acad. Sci.*, **1980**, 77:7380–7384.

(33) Lydersen, B. K. and Pettijohn, D. E., Human-specific nuclear protein that associates with the polar region of the mitotic apparatus: distribution in a human / hamster hybrid cell, *Cell*, **1980**, 22:489–499.

(34) Jansen, H., Boer, M., Otter, B., and Elwenspoek, M., The black silicon method IV: The fabrication of three-dimensional structures, in Silicon with high aspect ratios for scanning probe microscopy and other applications, *Proc. of 8th International Workshop on Micro Electrical Mechanical Systems*, 1995:88–93.

(35) Gunther, S., Alexander, R. W., Atkinson, W. J., and Gimbrone, M. A., Functional angiotensin II receptors in cultured vascular smooth muscle cells, *J. Cell Biol.*, **1982**, 92:289–298.

(36) Graham, F. L. and Van Dr Eb, A. J., A new technique for the assay of infectivity of human adenovirus 5 DNA, *Virology*, **1973**, 52:456–467.

(37) Chen, C. and Okayama, H., High-efficiency transformation of mammalian cells by plasmid DNA, *Molec. Cell. Biol.*, **1987**, 7:2745–2752.

(38) Felgner, P. L., Gadek, T. R., Holm, M., Roman, R., Chan, H. W., Wenz, M., Northrop, J. P., Ringold, G. M., and Danielsen, M., Lipofection: A highly efficient, lipid-mediated DNA-transfection procedure, *Proc. Nat. Acad. Sci.*, **1987**, 84:7413–7417.

(39) Pickering, J. G., Jeanowski, J., Weir, L., Takeshita, S., Losordo, D. W., and Isner, J. M., Liposome-mediated gene transfer into human vascular smooth muscle cells, *Circulation*, **1994**, 89:13–21.

(40) Tanner, F. C., Carr, D. P., Nabel, G. J., and Nabel, E. G., Transfection of human endothelial cells, *Cardiovasc. Res.*, **1997**, 35:522–528.

(41) Sanes, J. R., Rubenstein, J. L., and Nicolas, J. F., Use of a recombinant retrovirus to study post-implantation cell lineage in mouse embryos, *EMBO J.*, **1986**, 5:3133–3142.
(42) Block, P. C., Baughman, K. L., Pasternak, R. C., and Fallon, J. T., Transluminal angioplasty: Correlation of morphologic and angiographic findings in an experimental model, *Circulation*, **1980**, 61:778–785.
(43) Faxon, D. P., Sanborn, T. A., Weber, V. J., Haudenschild, C., Gottsman, S. B., McGovern, W. A., and Ryan, T. J., Restenosis following transluminal angioplasty in experimental atherosclerosis, *Arteriosclerosis*, **1984**, 4:189–195.
(44) Zuckerman, B. D., Weisman, H. F., and Yin, F. C. P., Arterial hemodynamics in a rabbit model of atherosclerosis, *Am. J. Physiol.*, **1989**, 257:H891–897.
(45) Berceli, S., Hemodynamics and atherogenesis: Low-density lipoprotein metabolism and endothelial cell morphology, Ph.D. dissertation, 1990, School of Engineering, University of Pittsburgh, Pittsburgh, Pennsylvania.
(46) Fry, D. L., Aortic evans blue dye accumulation: Its measurement and interpretation, *Am. J. Physiol.*, **1977**, 232(2):H204–H222.
(47) Fry, D. L., Mahley, R. W., and Suk, Y. O., Effect of arterial stretch on transmural albumin and evans blue dye transport, *Am. J. Physiol.*, **1981**, 240:H645–H649.
(48) Fry, D. L., Mahley, R. W., Weisgraber, K. H., and Suk, Y. O., Simultaneous accumulation of evans blue dye and albumin in the canine aortic wall, *Am. J. Physiol.*, **1977**, 233(1):H66–H79.
(49) Brant, A., Hemodynamics and mass transfer aspects of arterial disease, Ph.D. dissertation, 1986, School of Engineering, University of Pittsburgh, Pittsburgh, Pennsylvania.
(50) Fry, D. L., Cornhill, F. J., Sharma, H., Pap, J. M., and Mitschelen, J., Uptake of low-density lipoprotein, albumin, and water by de-endotheliallized *in vitro* minipig aorta, *Arteriosclerosis*, **1986**, 6:475–490.
(51) Couffinhal, T., Kearney, M., Sullivan, A., Silver, M., Tsurumi, Y., and Isner, J. M., Histochemical staining following LacZ gene transfer underestimates transfection efficiency, *Hum. Gene Ther.*, **1997**, 8:929–934.
(52) Sims, F. H., The internal elastic lamina in normal and abnormal human arteries: A barrier to the diffusion of macromolecules from the lumen, *Artery*, **1989**, 16:159–173.
(53) Sims, F. H., Discontinuities in the internal elastic lamina: A comparison of coronary and internal mammary arteries, *Artery*, **1985**, 13(3):127–143.
(54) Sims, F. H., Gavin, J. B., Vanderwee, M. A., The intima of human coronary arteries, *Am. Heart J.*, **1989**, 118:32–38.
(55) Schwartz, R. S., Huber, K. C., Murphy, J. G., Edwards, W. D., Camrud, A. R., Vlietstra, R. E., and Holmes, D. R., Restenosis and the proportional neointimal response to coronary artery injury: Results in a porcine model, *J. Am. Coll. Cardiol.*, **1992**, 19:267–274.
(56) Schwartz, R. S., Murphy, J. G., Edwards, W. D., Camrud, A. R., Vliestra, M. B., and Holmes, D. R., Restenosis after balloon angioplasty: A practical proliferative model in porcine coronary arteries, *Circulation*, **1990**, 82:2190–2200.
(57) Morimoto, S.–I., Mizuno, Y., Hiramitsu, S., Yamada, K., Kubo, N., Nomura, M., Yamaguchi, T., Kitazume, H., Kodama, K., Kurogane, H., Shimizu, Y., Mizuno, K., Chino, M., Watanabe, S., Ueda, T., Toyoda, M., and Sekiguchi, M., Restenosis after percutaneous transluminal coronary angioplasty: Histopathological study using autopsied hearts, *Jpn. Circ. J.*, **1990**, 54:43–56.
(58) Mintz, G. S., Pichard, A. D., Kent, K. M., Satler, L. F., Popma, J. J., and Leon, M. B., Axial plaque redistribution as a mechanism of percutaneous transluminal coronary angioplasty, *Am. J. Cardiol.*, **1996**, 77:427–430.
(59) Loree, H. M., Grodzinsky, A. J., Park, S. Y., Gibson, L. J., and Lee, R. T., Static circumferential tangential modulus of human atherosclerotic tissue, *J. Biomech.*, **1994**, 27(2):195–204.
(60) Lendon, C. L., Briggs, A. D., Born, G., Burleigh, M. C., and Davies, M. J., Mechanical testing

of connective tissue in the search for determinants of atherosclerotic plaque cap rupture, *Biochem. Soc. Trans.*, **1988**, 16(2):1032–1033.

(61) Neumann, E., Schaefer–Ridder, M., Wang, Y., and Hofschneider, P. H., Gene transfer into mouse lyoma cells by electroporation in high electric fields, *EMBO J.*, **1982**, 1:841–845.

(62) Fernandez–Ortiz, A., Meyer, B. J., Mailhac, A., Falk, E., Badimon, L., Fallon, J. T., Fuster, V., Cheseboro, J. H., and Badimon, J. J., A new approach for local intravascular drug delivery: Iontophoretic balloon, *Circulation*, **1994**, 89:1518–1522.

(63) Tsurumi, Y., Takeshita, S., Dongfen, C., Kearney, M., Rossow, S. T., Passeri, J., Horowitz, J. R., Symes, J. F., and Isner, J. M., Direct intramuscular gene transfer of naked DNA encoding vascular endothelial growth factor augments collateral development and tissue perfusion, *Circulation*, **1996**, 94:3281–3290.

(64) Tsurumi, Y., Kearney, M., Chen, D., Silver, M., Takeshita, S., Yang, J., Symes, J. F., and Isner, J. M., Treatment of acute limb ischemia by intramuscular injection of vascular endothelial growth factor gene, *Circulation*, **1997**, 96:II 382–II 388.

(65) Kneller, J. R., Wu, C. C., Vorp, D. A., Reed, M. L., Weiss, L. E., Borovetz, H. S., Watkins, S., Feldman, M. D., The use of microfabricated probes to penetrate the internal elastic lamina and intimal hyperplasia, *J. Cardiovasc. Diagn. Proc.*, **1999**, 16(2):37–50.